

Full temporal reconstruction of a lower order harmonic superposition

This content has been downloaded from IOPscience. Please scroll down to see the full text.

2007 New J. Phys. 9 232

(<http://iopscience.iop.org/1367-2630/9/7/232>)

View [the table of contents for this issue](#), or go to the [journal homepage](#) for more

Download details:

IP Address: 195.251.197.150

This content was downloaded on 15/11/2013 at 11:23

Please note that [terms and conditions apply](#).

Full temporal reconstruction of a lower order harmonic superposition

P Tzallas^{1,4}, E Skantzakis^{1,2}, E P Benis¹, C Kalpouzos¹,
G D Tsakiris³ and D Charalambidis^{1,2}

¹ Foundation for Research and Technology—Hellas, Institute of Electronic Structure and Laser, PO Box 1527, GR711 10 Heraklion, Crete, Greece

² Department of Physics, University of Crete, PO Box 2208, GR71003 Heraklion, Crete, Greece

³ Max-Planck-Institut für Quantenoptik, D-85748 Garching, Germany
E-mail: ptzallas@iesl.forth.gr

New Journal of Physics **9** (2007) 232

Received 2 March 2007

Published 17 July 2007

Online at <http://www.njp.org/>

doi:10.1088/1367-2630/9/7/232

Abstract. We demonstrate full spectral phase/amplitude distribution retrieval of an arbitrary superposition of the third and fifth harmonic fields of 800 nm central wavelength, fs laser radiation, through a cross-correlation approach. Using the retrieved distributions, the temporal profile of the total harmonic field has been reconstructed and found to be in agreement with simulations. The results reveal the suitability of the approach for full temporal characterization of a low-order harmonic superposition and thus for attosecond pulses.

⁴ Author to whom any correspondence should be addressed.

Contents

1. Introduction	2
2. The method	3
3. Results and discussion	5
4. Conclusions	7
Acknowledgments	9
References	9

1. Introduction

The determination of the entire spectral phase distribution of a high frequency radiation field is a key parameter and at the same time an important prerequisite for the precise reconstruction of radiation pulses with ultra-short duration, such as the recently generated single and trains of attosecond (asec) pulses. The latter are emitted during the nonlinear interaction of low frequency, many-cycle, intense fs laser radiation with a gaseous medium in a well established process known as harmonic generation [1]. The harmonic spectrum consists of a series of peaked frequency distributions around the odd harmonics of the driving laser field frequency and it exhibits a characteristic behaviour. The emission of harmonics with photon energies lower than the ionization energy of the nonlinear medium follows lowest order perturbation theory (LOPT) and thus the harmonic yield drops rapidly with harmonic order. Harmonics with photon energies higher than the ionization energy are emitted non-perturbatively exhibiting essentially constant yield with harmonic order up to the cutoff region. The underlying emission mechanism in this case is successfully described by the three step model [2]. According to the superposition principle of wave mechanics, asec light localization comes about when a number harmonics from the thus generated spectrum possessing proper phase and amplitude relations are superimposed in time and space.

The availability of UV/VUV pulses with duration of the order of 1 fs and more importantly of vacuum ultra-violet/extreme ultra-violet (VUV/XUV) asec pulses constitutes a breakthrough in the quest towards real time investigations of ultra-fast nuclear and electron dynamic processes of high interest to a number of different disciplines. Such investigations require in the first place, tractable and detailed pulse characterization measurements. While for intense asec pulse trains, approaches based on second-order XUV autocorrelation have been successfully implemented [3], in many cases XUV intensities are low, leaving no other option than the utilization of approaches based on cross-correlation measurements between the XUV and the driving laser radiation [4]–[6]. The most widely used cross-correlation techniques are the atomic streak camera [4], the RABBIT [5] and the CRAB–FROG [6]. Moreover, an XUV version of the SPIDER technique appeared recently in the literature [7].

The mapping of a spectral phase distribution can be achieved by measuring in a cross-correlation type of measurement the phase difference between all spectral components of the radiation to be characterized relative to the phase of a reference field. For the reconstruction of the temporal profile of a harmonic field E_q or a superposition of harmonic fields $\sum_q E_q$, the reference phase can be q -times the phase of a Fourier transform limited (FTL) fundamental laser field, q being the order of each harmonic of the superposition. This reference phase appears in

interaction schemes involving a linear driving process at frequency ω_q interfering with a nonlinear one at frequency $q\omega$, like those utilized in the phase sensitive coherent control technique [8]. In this technique, the yield of the interaction of matter with a bichromatic field is controlled through the relative phases of the two phase-correlated waves. In an inverse manner, measuring the variation of the interaction yield, information about the relative phases of the interfering interaction channels can be extracted and thus the field phase distributions may be retrieved.

We have recently proposed a cross-correlation approach based on this principle, i.e. on the ionization of atoms through two interfering pathways, namely single photon ($\hbar\omega_q$) and q -photon absorption ($q\hbar\omega$), that allows for full spectral phase distribution retrieval of ultra-short harmonic pulses [9]. Here, the term ‘full’ is justified as both the relative spectral phase between harmonics as well as between different frequency modes within the bandwidth of each harmonic are accounted for. A simplified ‘all optical’ version of the approach, measuring the total harmonic generation yield instead of ionization has been successfully implemented in reconstructing the temporal profile of FTL as well as chirped third harmonic fields of a Ti:sapphire laser produced in a gas medium [10]. In this modified version the ‘phase control’ is not only through quantum interference control of the induced atomic polarization, but also through macroscopically controlled phase matching between the interfering fields.

In the present work, we report on the determination of the complete spectral phase distribution of the superposition of the third and fifth harmonic fields generated in a gas medium from a Ti:sapphire laser system. This proof of principle experiment demonstrates that through this cross-correlation approach, apart from spatial effects [11], full spectral phase/amplitude distribution retrieval and thus complete temporal reconstruction of asec waveforms can be achieved.

2. The method

Harmonics are generated in a Xe gas cell, which henceforth will be called the first nonlinear medium (NLM1), by a 1 KHz repetition rate Ti:sapphire laser system, delivering pulses of 1 mJ energy/pulse and $\tau_L = 56$ fs duration at 800 nm carrier wavelength (figure 1). The generated harmonics co-propagate with the fundamental, entering a transmission grating Michelson interferometer described elsewhere [12]. The interferometer selects the third and fifth harmonic from the entire harmonic spectrum. The piezoelectric translation stage in the interferometer allows for the introduction of a variable delay (phase shift) between the fundamental and the two harmonic fields with a nominal step of ~ 20 asec and maximum linear displacement of $\sim 15 \mu\text{m}$. The three fields, with frequencies ω , ω_3 and ω_5 , are subsequently focused in a second Xe gas cell, which henceforth will be called the second nonlinear medium (NLM2). In NLM2, the harmonics are generated by the fundamental in the presence of the harmonic fields produced in NLM1. The superimposed third and fifth harmonic fields to be characterized are cross-correlated with the FTL laser field in three versus one and five versus one coupling schemes, respectively, as depicted in figure 2. In order for the fundamental laser pulse to be FTL in the NLM2 a pre-compensated fundamental pulse has been used. In the following discussion it is assumed that all interactions are within the LOPT and that the fundamental field $E_\omega(\omega, z, t)$ is FTL. In NLM2, assuming that the pulses are so long that time effects can be ignored and that the field is in steady-state within the interaction volume, the propagation equation for the slowly varying amplitude of any of the harmonic frequency components ω_q ($q = 3, 5$) within the spectral region of interest, results in

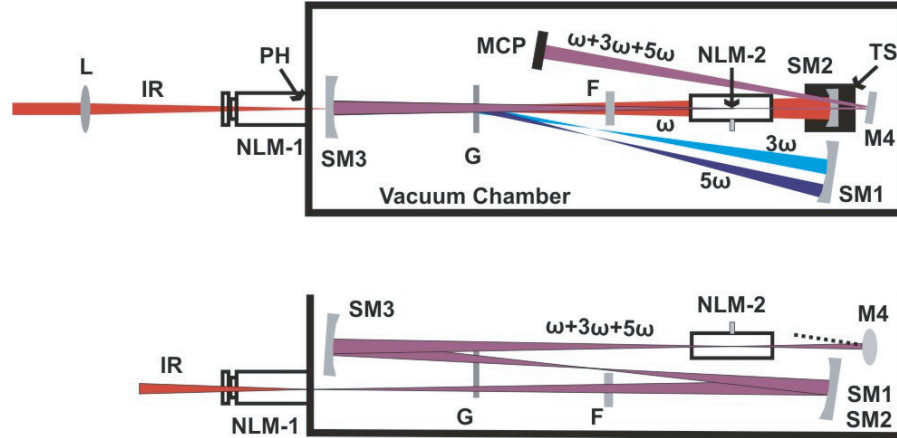


Figure 1. Top view (upper panel) and a side view (lower panel) of the experimental set-up. L: $f = 30$ cm focal length lens. NLM1 and NLM2: nonlinear medium (gas cell) 1 and 2. PH: pinhole. G: $600 \text{ lines mm}^{-1}$ fused Silica transmission grating. The grating is mounted on a translation stage. SM1, SM2 and SM3: $f = 30$ cm un-protected gold spherical mirrors. F: 3 mm thick BK7 filter. TS: translation stage. M4: un-protected gold flat mirror. MCP: microchannel plate detector.

a harmonic field at the exit of the NLM2

$$E_{\omega_q}(z = L) = E_{\omega_q}(z = 0) + A \int_0^L P(\omega_q, z, t) e^{-i\Delta k z} dz, \quad (1)$$

where $\Delta k = k_q - qk$ is the wavevector mismatch between the harmonic and the fundamental, $z = 0$ is the position of the entrance to the NLM2, and thus $E_{\omega_q}(z = 0)$ is the harmonic field entering this medium, i.e. the field produced in NLM1. L is the length of NLM2 and A is a constant. $P(\omega_q, z, t)$ is the polarization of the medium at ω_q , which in general consists of interfering nonlinear P^{NL} and linear P^{L} terms:

$$P(\omega_q, z, t) = P^{\text{NL}}(\omega_q, z, t) + P^{\text{L}}(\omega_q, z, t) = \chi^{(q)} E_{\omega}^q(z, t) + \chi^{(1)} E_{\omega_q}^{\text{NLM1}}(z, t), \quad (2)$$

where $\chi^{(q)}$ and $\chi^{(1)}$ are the nonlinear and linear susceptibilities at ω_q , respectively. Due to the resulting three interfering terms in equation (1), the emitted intensity at ω_q is

$$I_{\omega_q} = C + B \times \cos(\varphi_q(\omega_q) - q\varphi_L) \quad (3)$$

with C and B being constants and φ_q , φ_L the phases of the harmonic and fundamental fields, respectively. Introducing a variable delay τ between the two fields the measured intensity becomes oscillatory with τ and carries information about φ_q :

$$I_{\omega_q}(\tau) = C + B \times \cos(\varphi_q(\omega_q) - \omega_q \tau). \quad (4)$$

Note that, in this ‘all optical’ arrangement, even when the linear term in equation (2) becomes negligibly small, the measured signal carries the same phase information. This is not the case

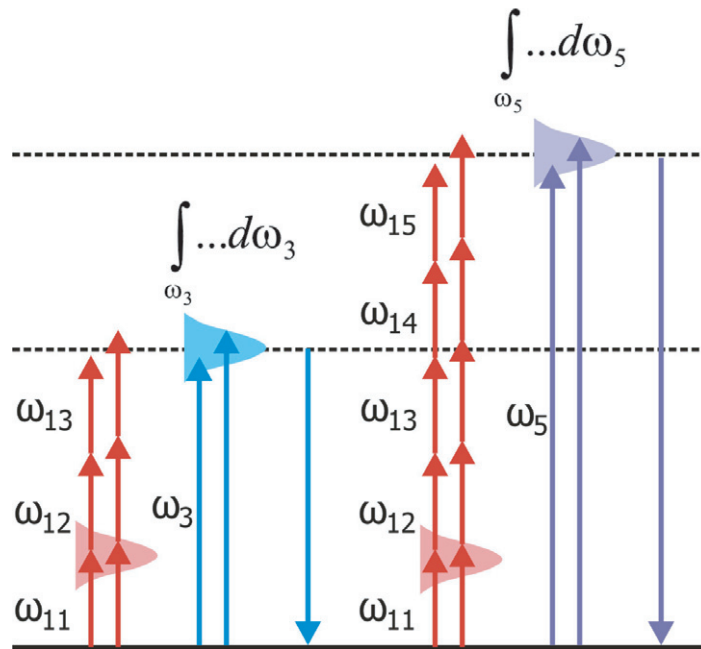


Figure 2. Coupling scheme in the NLM2. ω_{1i} , $i = 1 \dots 5$ denote the frequencies of the modes within the bandwidth of the fundamental. $\omega_{3,5}$ are the frequency distributions of the third and fifth harmonics, respectively. The double index for the fundamental frequency has been for simplicity omitted in the text, as the use of FTL pulses makes the explicit mode notation redundant.

when the measured quantity is ionization in the NLM2 [9] instead of harmonic generation, for which the two terms in equation (2) have to be comparable in strength.

For a polychromatic field, as is the case in the present experiment, the total harmonic signal at the exit of NLM2, spatially integrated and recorded through a microchannel plate (MCP) detector, is the incoherent sum of intensity contributions of the type of equation (4) from all the spectral components involved in the interaction, i.e.

$$I_{\text{TOTAL}}(\tau) \propto \sum_{q=3,5} \int_{\omega_q} B(\omega_q) \cos(\varphi_q(\omega_q) - \omega_q \tau) d\omega_q. \quad (5)$$

The summation, although redundant, is introduced in order to denote that the harmonic field is spectrally localized around the third and fifth harmonic of the fundamental. A Fourier transform of the cross-correlation signal of equation (5) yields the entire spectral phase distribution for the two harmonics under investigation.

3. Results and discussion

A numerical simulation of the experiment, utilizing a three-dimensional (3D) ray tracing code and a code accounting for the dispersion introduced by propagation in dispersive elements, has

been performed⁵, and the results are compared with the measurements. For the 3D ray tracing, the 3D capabilities of the OPTICA[®] package of MATHEMATICA[®] have been used. An analytical code has been developed in MATHEMATICA[®] based on the Sellmeier dispersion formula [13], in order to determine the group velocity dispersion (GVD) introduced through propagation and thus the pulse duration of the fundamental and the harmonics. Using these codes, we have accounted for all effects of the beam propagation through all dispersive elements of the set-up, diffraction at the grating, the reflection by the tilted mirrors and the focusing characteristics of the beams in NLM2. Furthermore, we can also assess the geometrical aberrations introduced by the optical design used. In the analysis, parameters such as distances, focal lengths, tilt angles are equated to the experimental ones. From these calculations the complex fields $E_\omega(\omega, t)$ and $E_{\omega_q}(\omega_q, t)$ ($q = 3, 5$) of the fundamental, third and fifth harmonic respectively at the entrance of NLM2 have been extracted. The cross-correlation trace shown in the inset of figure 3(a) has been simulated for a delay τ range from -25 to 25 fs applying the interference formula:

$$I(\tau) \propto \int dt \left[\left| D_1 E_\omega^3(t - \tau) e^{i3\omega(t-\tau)} + D_3 E_{\omega_3}(t) e^{i(\omega_3 t + a t^2)} \right|^2 + \left| D_1 E_\omega^5(t - \tau) e^{i5\omega(t-\tau)} + D_5 E_{\omega_5}(t + \Delta\tau) e^{i(\omega_5(t+\Delta\tau) + b(t+\Delta\tau)^2)} \right|^2 \right], \quad (6)$$

where τ is the variable delay, E_ω , E_{ω_3} and E_{ω_5} the field envelopes of the fundamental, third and fifth harmonic respectively, a and b the chirp values of the two harmonic fields and $\Delta\tau$ the delay between the third and fifth harmonic pulse respectively, introduced through the dispersive elements as derived from the above mentioned calculations. D_i ($i = 1, 3, 5$) are constants, the values of which are chosen so that the amplitudes of the interfering terms in each of the two interference pairs are equal and the ratio of the maxima of the two superimposed interferograms is equal to the experimental ratio of the intensities of the fifth to the third harmonic. Note that equation (6) is equivalent to (5).

By a Fourier transform of the trace, the spectral phase distribution of the superposed third and fifth harmonic field in the 50 fs time gate window has been obtained (figure 3(a) and (b)). The third harmonic phase shows no frequency dependence, while the fifth harmonic phase depicts a quadratic dependence on the frequency. The latter originates from the linear chirp induced by the propagation of the radiation through the dispersive optical materials, which for the third harmonic is negligible. The harmonic spectral amplitudes were assumed to be equal to the experimental values. Using the above spectral phase and amplitude distributions the simulated harmonic field superposition has been reconstructed. The pulse duration of the reconstructed temporal profile is found to be close to the FTL value of 32 fs for the third harmonic pulse and 270 fs for the chirped fifth harmonic pulse. The temporal separation between the third and fifth harmonic field, induced by the propagation of the fields in the dispersive materials, is partially compensated in the experiment by changing the grating position in the interferometer [12] (and see footnote 5). In the simulation, this temporal separation between the two harmonic pulses is arbitrarily set to 120 fs.

The measured cross-correlation trace for the superposed third and fifth harmonic fields is shown in the inset of figure 4(a) in the range of -25 to 25 fs. The solid black lines in figure 4(a) and (b) depict the spectral phase distribution retrieved through the Fourier transform of the measured cross-correlation trace which is found to be in very good agreement with the simulated one. Here,

⁵ Detailed analysis of the calculations and description of the experimental apparatus will be given in forthcoming publication by E Skantzakis *et al.*

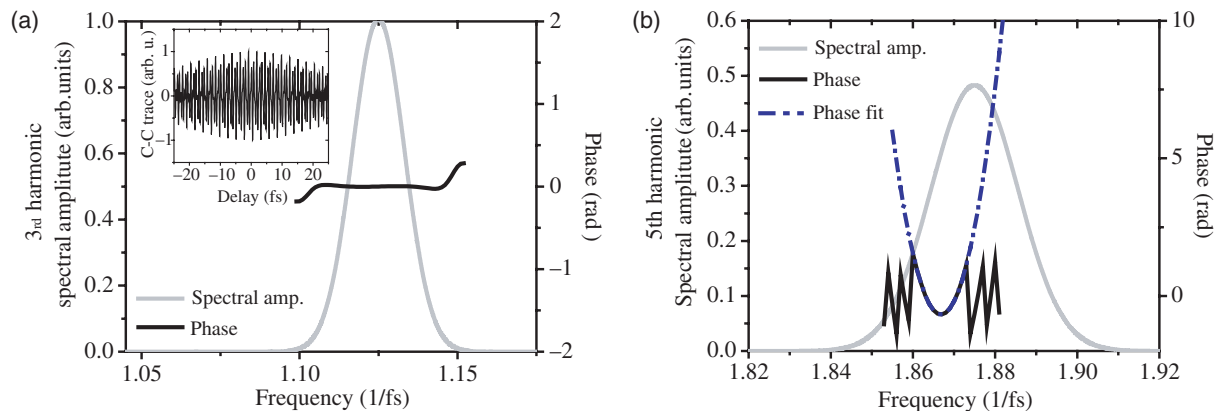


Figure 3. (a) Inset: the simulated cross-correlation trace between the fundamental (IR) and the superposed third and fifth harmonic fields. (a) and (b): Fourier transform spectra. Grey line: spectral amplitudes of the third and fifth harmonic. Black line: extracted spectral phase distribution of the simulated superposed third and fifth harmonic field. Dash-dot line: parabolic fit of the central part of the spectral phase distribution.

the Fourier transform procedure has been corrected for the contribution of the 50 fs gate window. Using a modified geometry of the experimental set-up [9], the first-order autocorrelation trace has been recorded, from the Fourier transform of which the spectral amplitudes of the harmonics have been obtained (figure 4(a) and (b)). The spectral widths of the harmonics are found to be in good agreement with those expected from LOPT. From the retrieved spectral phase and amplitude distribution, the superposed harmonic field has been fully reconstructed and is shown in figure 5(a) and (b). The pulse duration of the third and fifth harmonic is found to be 31 ± 5 and 260 ± 40 fs, respectively. These values are in agreement with those from the simulation. Due to an incomplete compensation through the displacement of the grating, there is a remaining time delay of 65 fs between the two fields. Figure 5(b) shows the interference structure of the superposed third and fifth harmonic field. The low contrast of the beating is due to the significantly different amplitudes of the third and fifth harmonic. This result indicates that the approach is not restricted to harmonic fields with almost equal intensities, being sensitive also to a weak signal modulation.

4. Conclusions

Concluding, the full spectral phase and amplitude distribution of an arbitrary superposition of the third and fifth harmonic fields of 800 nm central wavelength, fs laser radiation, has been measured through a cross-correlation approach. Using the measured spectral phase/amplitude distributions, the temporal profile of the superposed harmonic field has been reconstructed and found to be in agreement with simulations. The results demonstrate the suitability of the approach for full temporal characterization of broad band short wavelength radiation, such as high-order harmonic superposition and thus of asec pulses. The technique is rigorously applicable, as long as harmonic generation in the NLM2 can be treated by LOPT. This sets an upper limit to the

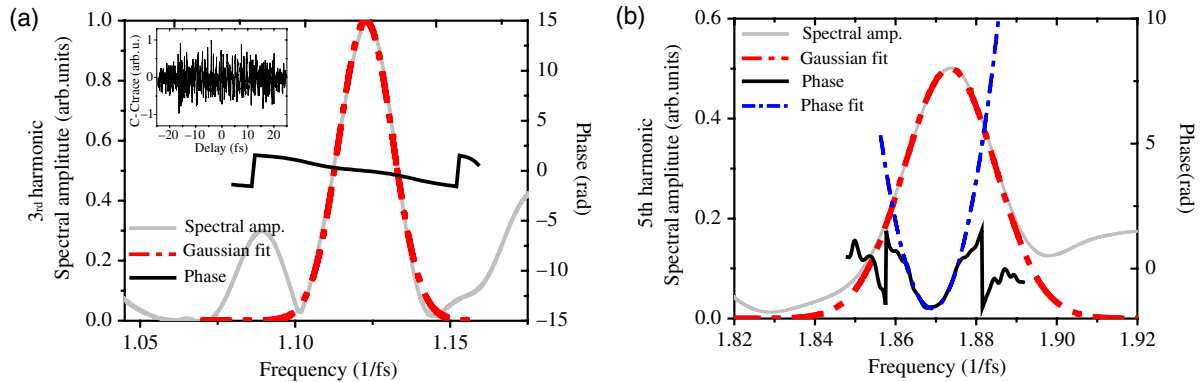


Figure 4. (a) Inset: the recorded cross-correlation trace between the fundamental and the superposed third and fifth harmonic fields. (a) and (b): Fourier transform spectra. Grey line: spectral amplitudes of the third and fifth harmonic extracted by the Fourier transform of the first-order AC trace of the third and fifth harmonic fields. Black line: measured spectral phase distribution of the superposed third and fifth harmonic field. Note that there is no phase shift between the two phase axes scales. Thus, the phases between the two harmonics and within the bandwidth of each harmonic are simultaneously determined. Red dash-dot line: Gaussian fits. Blue dash-dot line: parabolic fit of the central part of the spectral phase distribution.

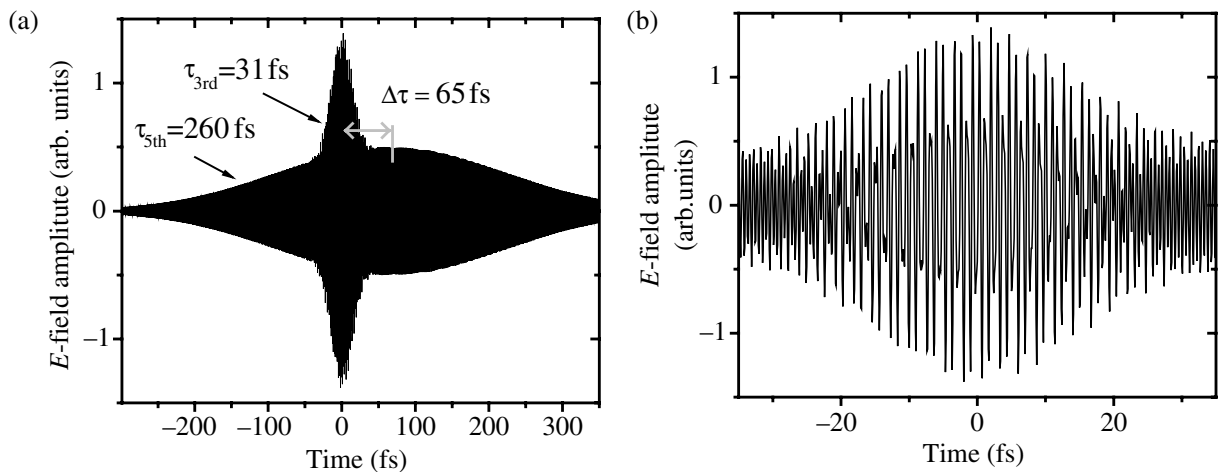


Figure 5. (a) The reconstructed field of the third and fifth harmonic superposition. (b) Part of the reconstructed field showing in detail the interference structure of the superposed third and fifth harmonic field.

order of the harmonics that can be characterized. Using He as NLM2, phases of fields including harmonics up to the 15th of the 800 nm laser radiation can be retrieved. Utilizing Xe as NLM1, XUV radiation with a bandwidth of ~ 10 eV and slowly varying spectral amplitude can be treated and thus asec pulses as short as ~ 250 asec can be fully reconstructed. For the characterization of waves with wavelengths below the LiF limit a free standing transmission grating [12] or an alternative cross-correlation arrangement has to be used. Extension of the approach to photon

energies larger than the ionization potential of He is subject to a beyond LOPT validity assessment of the approach for each specific case, through theoretical modelling [14]. As an IR-UV/VUV cross-correlation technique, based partially on quantum interference effects, the present approach is related to the RABBIT approach [5], with the advantage (albeit within the limitations discussed above) of accounting for the chirp also within the bandwidth of the individual harmonics. The method is applicable as well to coherent broad band continua (i.e. to isolated asec pulses) and can be further extended to use iterative algorithms fitting trial waveforms to measure traces as the FROG [15] and CRAB-FROG [6] techniques do. Moreover, as an ‘all optical’ method it is simpler to implement, not requiring tedious energy resolved measurements.

Acknowledgments

This work is supported in part by the European Community’s Human Potential Program under contract MRTN-CT-2003-505138 (XTRA); MTKD-CT-2004-517145 (X-HOMES); the Ultraviolet Laser Facility (ULF) operating at FORTH-IESL (contract no. HPRI-CT-2001-00139) and the P14 COST programme. Discussions with E Papalazarou are acknowledged.

References

- [1] Ferray M *et al* 1988 *J. Phys. B: At. Mol. Opt. Phys.* **21** L31
McPherson A *et al* 1987 *J. Opt. Soc. Am. B* **4** 595
L’Huillier A and Balcou Ph 1993 *Phys. Rev. Lett.* **70** 774
- [2] Corkum P B 1993 *Phys. Rev. Lett.* **71** 1994
Lewenstein M *et al* 1994 *Phys. Rev. A* **49** 2117
- [3] Tzallas P *et al* 2003 *Nature* **426** 267
Nikolopoulos L A A *et al* 2005 *Phys. Rev. Lett.* **94** 113905
Nabekawa Y *et al* 2005 *Phys. Rev. Lett.* **94** 043001
Nabekawa Y *et al* 2006 *Phys. Rev. Lett.* **97** 153904
- [4] Drescher M *et al* 2001 *Science* **291** 1923
- [5] Paul P M *et al* 2001 *Science* **292** 1689
Mairesse Y *et al* 2003 *Science* **302** 1540
- [6] Mairesse Y and Quere F 2005 *Phys. Rev. A* **71** 011401(R)
- [7] Cormier E *et al* 2005 *Phys. Rev. Lett.* **94** 033905
- [8] Shapiro M *et al* 1988 *Chem. Phys. Lett.* **149** 451
Chen C *et al* 1990 *Phys. Rev. Lett.* **64** 507
Bandrauk A D *et al* 1992 *Chem. Phys. Lett.* **200** 399
Nakajima T *et al* 1993 *Phys. Rev. Lett.* **70** 1081
Nakajima T *et al* 1993 *Phys. Rev. A* **50** 595
Dupont E *et al* 1995 *Phys. Rev. Lett.* **74** 3596
Sheehy B *et al* 1995 *Phys. Rev. Lett.* **74** 4799
Langchi Zhu *et al* 1995 *Science* **270** 77
Langchi Zhu *et al* 1997 *Phys. Rev. Lett.* **79** 4108
Cavalieri S *et al* 1997 *Phys. Rev. A* **55** 2941
Xenakis D *et al* 1998 *Opt. Commun.* **152** 83
Karapanagioti N E *et al* 1996 *J. Phys. B: At. Mol. Opt. Phys.* **29** 3599
Charron E *et al* 1993 *Phys. Rev. Lett.* **71** 692
Cormier E *et al* 1997 *J. Phys. B: At. Mol. Opt. Phys.* **30** 3095
Andiel U *et al* 1999 *Europhys. Lett.* **47** 42

- [9] Hertz E *et al* 2001 *Phys. Rev. A* **64** 051801R
- [10] Papalazarou E *et al* 2006 *Phys. Rev. Lett.* **96** 163901
- [11] Gaarde M B and Schafer K J 2002 *Phys. Rev. Lett.* **89** 213901
Kazamias S *et al* 2004 *Phys. Rev. A* **69** 063416
Nikolopoulos L A A *et al* 2005 *Phys. Rev. Lett.* **94** 113905
- [12] Goulielmakis E *et al* 2002 *Appl. Phys. B* **74** 197
- [13] Tatian B 1984 *Appl. Opt.* **23** 4477
- [14] Makris M *et al* 2002 *Phys. Rev. A* **66** 053414
- [15] Trebino R *et al* 1997 *Rev. Sci. Instrum.* **68** 3277